MULTISCIA JOURNALS PUBLISHERS

FRONTIERS IN MATERIAL SCIENCE AND NANOTECHNOLOGY

ISSN: (3065- 4114)

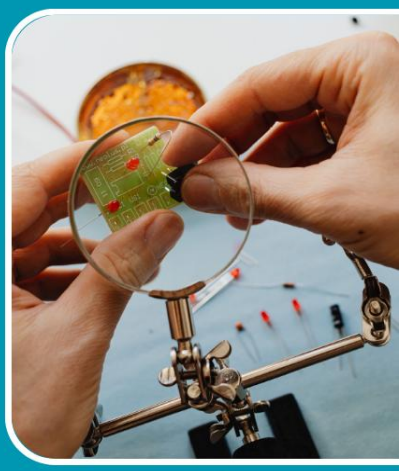

editor.fmsnt@gmail.com

https://multisciajournals.com/journals/index.php/fmsnt

Solar-Activated Ag/ZnO Nanostructures for Plasmon-Mediated Photocatalysis: Organic Pollutant Degradation in Water

Khannakar PK*

Department of Material Science and Nanotechnology

Article Info

Received: 23-06-2025 Revised:20-07-2025 Accepted:03-08-2025 Published:15-08-2025

Abstract

Effective treatment employing an in-situ generated Ag/ZnO nanocatalyst is the subject of this investigation. In the process of making catalysts, the environmentally friendly surfactant starch was used to create plate-shaped zinc oxide nanoparticles. X-Ray Diffraction research confirms that the as-synthesized catalyst contains hexagonal ZnO and fcc silver. Both the ZnO and Ag/ZnO crystal structures were shown to be correct by XRD examination, with d-spacings of 0.26 nm and 0.234 nm, respectively. The presence of starch allowed FESEM, EDX, and TEM to reveal a spherical yet flat plate type shape. The composition's oxygen richness was confirmed by XPS, and band gap energies were shown to decrease with increasing silver loading using UV-Vis spectrophotometry. Photographs of the plasmonic catalysts' photocatalytic action were taken using sunlight. Organic dyes including p-nitrophenol (PNP), methylene blue (MB), rhodamine B (RhB), methyl orange (MO), and bromophenol blue (BPB) were fully degraded in aqueous solutions as seen by absorption spectroscopy. After the third recycle, the catalyst's properties remained unchanged. This simple catalyst might be a quick and easy technique to cure effuently under the sun.

Keywords: Plasmonic Photocatalysis; Semiconductor; Advanced Oxidation Process; Dye Degradation

Introduction

Since Fukushima and Honda's 1971 achievement of water splitting with TiO2 under light irradiation [1], researchers have extensively studied the photocatalytic activity of semiconductor materials. Since they are readily available, non-toxic, thermally and chemically stable, and have several uses (e.g., photo-degradation of organic pollutants [5,6], artificial photosynthesis [7], and water splitting [8]), semiconductors TiO2 and ZnO have garnered a lot of attention as photocatalytic reaction materials. Although ZnO and TiO2 have a comparable band gap energy (~3.2 eV), ZnO is better in degrading water pollutants [9]. Photocatalytic degradation processes may be carried out more efficiently by ZnO due to its lower electric potentials in the valence and conduction bands (-0.45 to 2.75 eV) compared to TiO2 (-0.1 to 3.1 eV) [10,11]. As an additional benefit, ZnO has more quantum efficiency than TiO2 when used as a photocatalyst to degrade contaminants in water [12]. Since photocatalytic degradation converts organic contaminants to carbon dioxide and water without producing any hazardous by-products, it is an eco-friendly process [13,14]. It is common practice to conduct laboratory photocatalytic reactions under xenon lamp illumination rather than in natural sunlight to ensure accurate catalyst performance testing. Direct sunshine, of which 50% is UV radiation, is ideal for conducting degradation studies, as it improves the process's attractiveness. The band-gap properties of ZnO restrict its UV activity to the 3–4% solar spectrum. The optical properties of ZnO need to be adjusted within the visible range, namely between 400 nm and 700 nm, in order for it to function as an efficient catalyst in the visible area, which receives around 44% of the sun's energy [15]. Creating structural flaws [16], synthesising particles of varied morphologies, doping, etc., are only a few of the many strategies used to change the band-gap of ZnO. Nanorods [18], nanoflowers [19], nanowires [20], and nanosheets [21] are just a few examples of the different shaped and sized nanoparticles that have been synthesized to enhance their crystalline quality and make them more useful as visible light photocatalysts. One eco-friendly and efficient surfactant alternative is bio-polymers like starch, which are used to regulate the size and form of particles. Starch is a green precursor and an economically feasible choice for producing ZnO; its polymeric nature reportedly serves as a template for the development of highly crystalline nanoparticles [22-25].

One of the most effective semiconductor photocatalysts, TiO2 has been employed widely according to literature sources. The main obstacle to achieving high photocatalytic effectiveness against pollutants is the rapid recombination of charge carriers when exposed to light. The quantum efficiency of photocatalysis is diminished due to the quicker kinetics of electron and hole pair recombination. It is crucial to reduce the recombination rate to increase the photocatalysis efficiency. Changing the surface charge, functionality, reactivity, and stability of the photocatalyst may alleviate this photocorrosion issue. Several papers have detailed the restriction of photocorrosion by surface modification; here we will examine a few key examples. Zhu et al. [25] successfully reduced photocorrosion by combining ZnO with graphite-like carbon. The improvement of catalytic activity and reduction of photocorrosion caused by surface modification is detailed in another study on photoelectrochemical water splitting using carbon and nitrogen co-treated ZnO nanorod arrays. Photocatalysis demonstrated promising outcomes when ZnO was coupled with carbon materials and decreased graphene oxide, leading to improved photocatalytic activity and reduced photocorrosion [26]. You may also think about doping ZnO [26] with metals [27], non-metals [28], other chemicals [29], or semiconductor materials [15] to boost its visible range photocatalytic activity. The most desirable of these is the use of noble metal doping, such as Ag or Au, because of light-induced photoluminescence (LSPR), a feature that is exclusive to noble metal conduction band electrons. Doping with noble metals, such as silver, reduces electron-hole recombination [30] by creating a Schottky circuit; catalysts doped with noble metals are often called plasmonic photocatalysts [31,32]. Multiple studies have examined Ag-doped ZnO, (e.g. By tracking the degradation response of

Rhodamin 6G (R6G), Georgekutty et al. [33] documented the visible light performance of Ag doped ZnO particles. While Mondal [34] et al. monitored a spectrum of dyes to study the direct sunlight performance of ZnO photocatalysts doped with Au, the degradation efficiency was not appealing. Using starch as a surfactant, Zhang et al. [22] created microporous ZnO with high crystallinity that exhibited remarkable UV catalytic activity. Research showed that semiconductors with a high oxygen concentration were more effective as visible light photocatalysts. Even though Ag/ZnO may be synthesized in a single pot, a great alternative would be to precipitate the silver nanoparticles onto the surface, as this would allow for more control over the particle concentration. Here, the authors expand their work in photocatalysis, building on their prior demonstrations of the manufacture and uses of ZnO, TiO2, and silver nano-particles [22]. Sintering starch at a lower temperature to preserve oxygen-rich surfaces is fundamental to the current study's creation of a highly solar-active silver-doped ZnO photocatalyst. Methylene Blue was selected as the principal dye for the purpose of studying the photocatalytic performance. Additional organic dye degradation processes were seen for p-nitrophenol, bromophenol blue, methyl orange, and Rhodamine B. Solar degradation of p-nitrophenol using Ag doped ZnO is described in this study for the first time, as far as we are aware.

Experimental

Materials

All reagents used were of analytical grade and were purchased from commercial sources. The water used for the experiment is ultrapure water from Millipore Direct Q 3UV purifier system.

Instrumentation

The Bruker A8 advanced with monochromatized CuKα radiation, an accelerating voltage of 40 kV, and an applied current of 20 mA were used to conduct the powder X-Ray diffraction. To determine the nanocrystal composition, a supra 40, Carl Zeiss Pvt. Ltd. Instrument, and an Oxford Link, ISIS 300 were used for field emission scanning electron microscopy (FESEM) and energy dispersive atomic scattering (EDAX), respectively. Researchers used an Agilent Cary Eclipse fluorescence spectrophotometer to measure photoluminescence. Transmission Electron Microscope (TEM) images were taken by TECHNAI G2 instrument. The ESCA-3000, manufactured by VG Microtech UK, was used for X-Ray Photoelectron Spectroscopy (XPS), which used Mg Kα and Al Kα sources. We used a Specord 210 plus (Analytik Jena) for all of our ultraviolet-visible spectroscopic investigations. A Lutron LX-101A light meter was used to measure the intensity of the sunshine. Direct sunshine with an average intensity of around 86,500 LUX, as measured by a LUX meter, was used to conduct the photocatalytic activities.

Synthesis of ZnO nanoparticles

Zinc Nitrate 30.00g is added to 0.5% starch solution [11] and the mixture was kept under constant stirring for an hour. After complete dissolution of the zinc nitrate, temperature was increased to 60 °C and 600 ml NaOH solution in water (0.2 M) was added to the reaction mixture. The mixture was further stirred at same temperature for another 4 hrs. The overall mixture was kept for cooling and ageing overnight. The suspension was centrifuged to collect white precipitate which was washed with ethanol and distilled water twice. White powder so-collected was dried in an oven at 80 °C for 3-5 hrs.

Synthesis of Ag/ZnO nano catalyst

1.0g of ZnO nanoparticles were taken and dispersed in 100 ml ethanol *via* sonication process for 30 minutes. $AgNO_3$ (40 mg) was suspended in above solution for preparation of Ag/ZnO 1. The solution was stirred for 3 hours at a temperature of 45 °C to obtain a brownish yellow precipitate. The precipitate was centrifuged, collected and washed with ethanol and DI water. Similarly, Ag/ZnO 2 was prepared by adding 160 mg of $AgNO_3$ to the solution/suspension containing same amount of ZnO.

Photocatalytic study

Seeing how quickly methylene blue dye degraded in sunshine allowed us to gauge the Ag/ZnO composition's photocatalytic activity. A solution of methylene blue in water with a concentration of 0.02 mM was made using distilled water. A final reaction solution (1g/L) was prepared for photocatalytic assessment by dispersing 30 mg of bare ZnO or Ag/ZnO catalysts into 30 mL of methylene blue solution. For 20 minutes, the solutions were agitated vigorously and held in the dark until the MB and catalyst surfaces reached an adsorption equilibrium. The mixture was stirred occasionally when left in direct sunshine. Following the reaction, the sample's UV/Vis spectra were recorded by centrifuging 2 mL of solution every 20 minutes. Various concentrations of catalysts were used to repeat the operation. The following substances were also tested in the same manner: p-nitrophenol, Rhodamine B (RhB), Methyl Orange (MO), and Bromophenol Blue (BPB).

Results and Discussion

White crystalline nanoparticles of ZnO is formed as the result of the reaction.(A in Figure 1). During reaction Zn ions of Zinc Nitrate interact with OH radicals of starch networks, which is an important component of the system [24]. The zinc oxide formed get converted to ZnO nanoparticles by heat treatment at 100-200 °C. The nitrate group get decomposed as NO_2 and Oxygen.

The typical reaction can be expressed as:

$$Zn(NO_3)_2.\ 6\ H_2O + 2NaOH \rightarrow 2NaNO_3\ (aq.) + Zn(OH)_2 + 6H_2O \quad .....(1)$$

$$Zn\ (OH)_2 \rightarrow ZnO + H_2O \quad .....(2)$$

Figure 1: As-synthesized ZnO (A), Ag/ZnO **1** (B) and Ag/ZnO **2** (C) nanoparticles

Suspension of ZnO particles capped with starch was made in ethanol and $AgNO_3$ was added to it for loading of silver particles via reduction of silver ions. The process involves reduction of silver salt by the ethanol solution whereby Ag particles are formed on the surface of ZnO. Ethanol is known to be a mild reducing agent and formations of silver nano-particles have been reported by ethanol reduction process by others also [35]. The color changes from white to mild yellow and/or yellow brown for the final silver doped zinc oxide powders (B, C in Figure 1). The typical chemical reaction mechanism could be explained as below;

$AgNO_3 + C_2H_5OH + ZnO \rightarrow Ag^+ + NO_3^- + ZnO + C_2H_5O^- + H^+$ .....(3)

$Ag^+ + e^- + ZnO \rightarrow Ag^0$ /ZnO .....(4)

The so-generated powders were analyzed by several modern tools e.g. XRD, SEM, TEM, XPS, UV-Vis and PL spectroscopy.

XRD Measurements

A powder X-ray diffraction (PXRD) analysis was performed on the as-prepared samples to ascertain their crystallinity, phase, and purity. As illustrated in Figure 2a, the XRD patterns of the ZnO and ZnO/Ag particles were found. The hexagonal ZnO structure has ten significant peaks at certain 2θ values: 31.82, 34.47, 36.29, 47.56, 56.53, 62.89, 66.35, 67.96, 69.15, 72.56, and 77.46º. These peaks correspond to the (100), (002), (101), (102), (110), (103), (200), (112), (201), and (202) crystal planes, respectively [22]. There are no structural changes owing to silver doping, since the same peaks present in the XRD pattern of Ag/ZnO. However, the pattern also exhibits peaks for fcc Ag. An good proof of the synthesis of silver at ZnO was provided by a peak at 2θ 38.45º, which is caused by the presence of the (111) crystal plane of silver particles on the surface of the material [18]. The XRD pattern shows a very faint hump, and the peak at 2θ 44.27º for (200) is also evident, while the peak at 2θ 64.60º for (220) is less distinct. The crystal planes of fcc metallic Ag are not very obvious. Figure 2b shows that in the presence of silver, there is a little red shift in the 2 theta values of the ZnO peaks, which may be the result of intera-the creation of a Schottky connection between the silver and the ZnO matrix [36]. Using the Debye-Scherrer equation [22], we were able to determine that the nanoparticles were 21.6 nm in size. Thanks to the incorporation of Ag particles into the matrix, the crystalline size of Ag/ZnO increased slightly but noticeably [37]. With an estimated silver particle size of 18.9 nm, either on the surface or in the ZnO matrix, the metal is likely to be adsorbed on the material. At a 2θ value of 34.47º, the lattice gap between the 002 plane and the other plane in ZnO is 0.26 nm. For 111 silver planes at a 2θ value of 38.45º, the same is true for the silver contained in the Ag/ZnO catalyst: 0.234 nm. The lattice spacings of the two materials are in good agreement with the stated values, which verifies the nanoparticles' high quality and their real crystal planes and structure [17]. The availability of oxygen vacancies inside the ZnO crystal structure is a key factor in determining its catalytic activity. Reports in the literature verified the presence of oxygen vacancies in this particular instance [37].

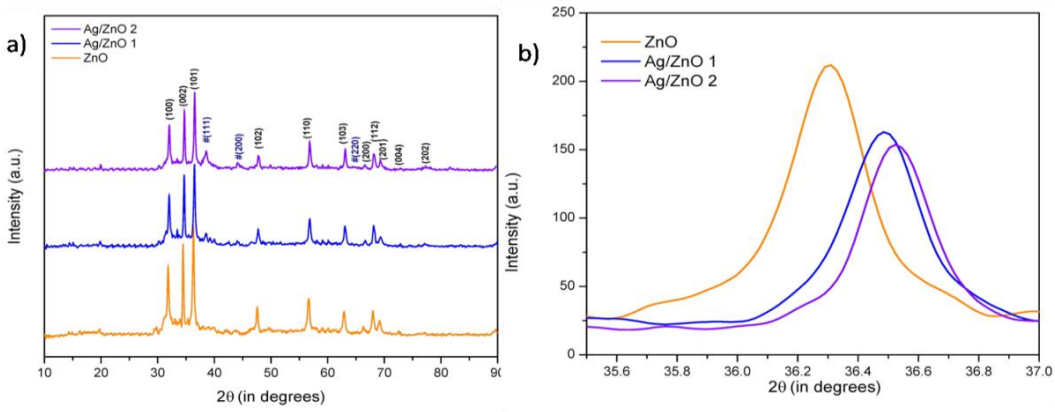

Figure 2: XRD patterns of various samples (a) ZnO and Ag/ZnO (b) 101 plane of same.

SEM/EDAX Analysis

Using scanning electron microscopy (SEM) examination, the shape of the ZnO particles and their distribution on the matrix's surface were examined (Figure 3). The SEM picture shows that the ZnO matrix has a plate-like morphology that is flaky and more or less tubular in form.

According to reports, energy harvesting processes may benefit from this mixed elongated shape [38]. The Ag-doped ZnO appeared as spherical flakes on the plate surface; these particles are no longer tubular but rather elongated, preserving the powder's mixed shape. Ag nanoparticles are evenly distributed throughout the surface of the ZnO nanoparticles. The higher concentration sample clearly shows more Ag particles than the lower concentration one.

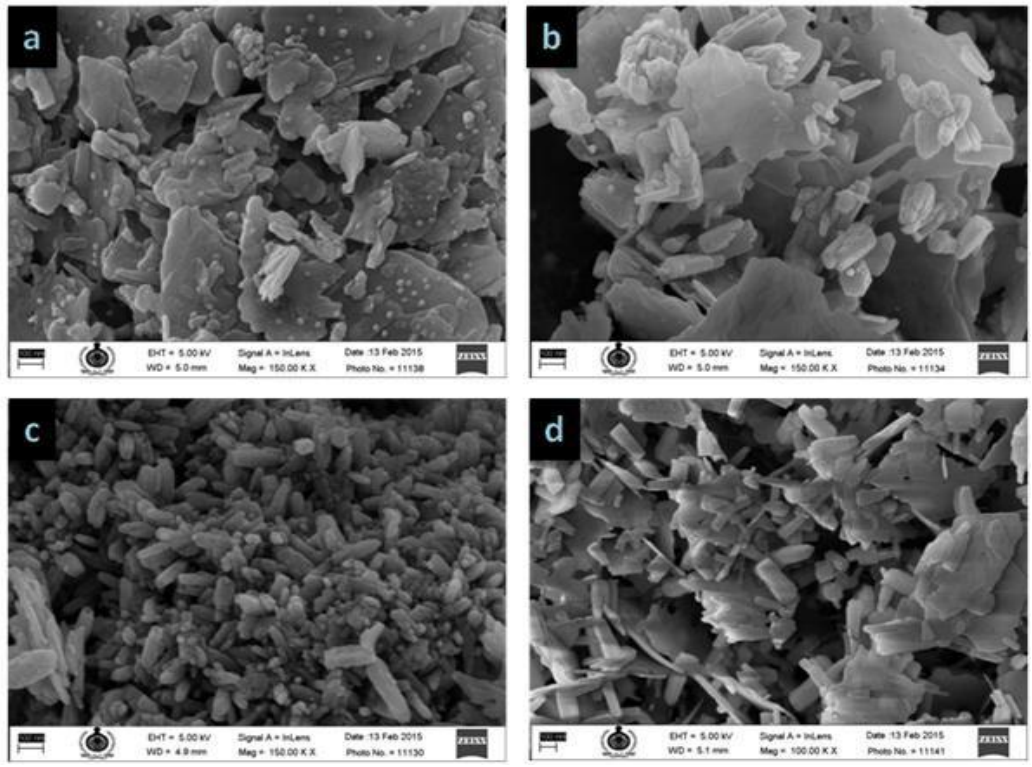

Figure 3: SEM of as-prepared a) Ag/ZnO 2; b, c) Ag/ZnO 1; d) ZnO (scale bar 100 nm)

Two clear silver percentages could be established with the help of EDAX analysis (Figure 4) e.g. the experiment conducted with lower concentration (40 mg) of silver salt resulted in close to 1% (0.89%) Ag loading on ZnO. However sample prepared with large concentration (160 mg) of $AgNO_3$ showed about 4% (3.89%) of Ag loading (Table 1). It is clear from EDAX analysis that only approximately 1 and 4% loading was completed. This indicates that, ethanolic reduction is indeed slow and during the reaction time, only about 40% much reduction was possible. It is found that Zn:O ratio is non-stoichiometric which can be because of the presence of starch thereby giving oxygen rich surfaces. It has been already described that oxygen rich TiO_2 is more effective as a photocatalyst [2]. In the present case too, this may stand valid for effective photo degradation of the organic during the photocatalytic process.

EDAX	ZnO		Ag/ZnO 1		Ag/ZnO 2	
Element	Weight %	Atomic %	Weight %	Atomic %	Weight %	Atomic %
O K	42.13	74.84	34.41	68.31	34.81	69.09
Zn K	57.87	25.16	64.70	31.43	61.27	29.76
Ag L	--	--	0.89	0.26	3.92	1.15

Table 1: Elemental composition from EDAX analysis

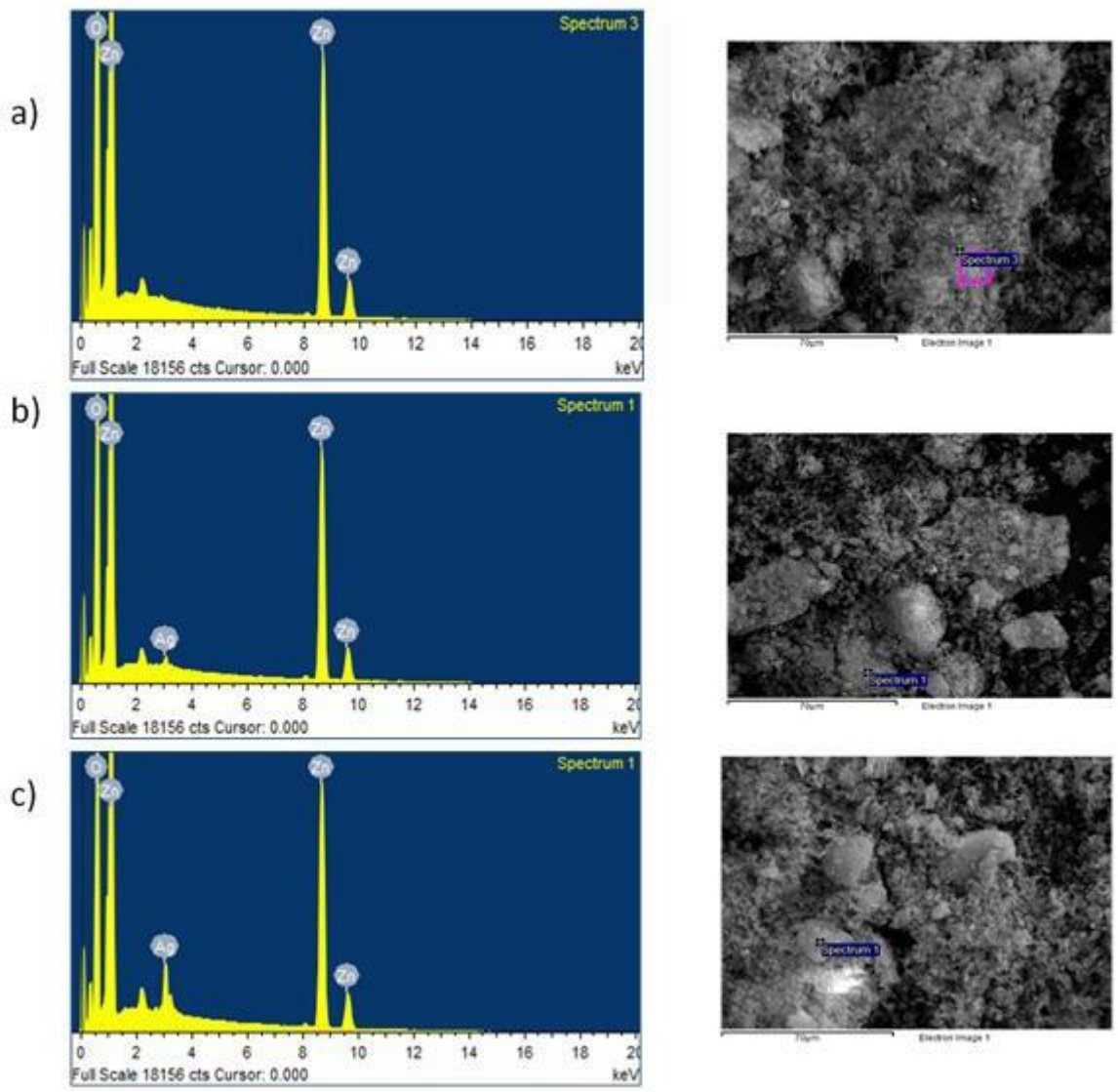

Figure 4: EDAX spectrum of a)ZnO b)Ag/ZnO 1 c)Ag/ZnO 2

SEM/EDAX Analysis

In the TEM images, the sample showed large plate and flaky appearance. The matrix plates (starch) are about 150-200 nm in length and about 20 nm in width. However uniformly distributed much smaller particle of ZnO can be considered due to presence of starch as overall matrix (Figure 5). The dark spots observed are due to homogeneously distributed silver nanoparticles on the surface of ZnO with the particle size of 15-20 nm. It is seen that ZnO is mostly appear as rod shape which match well with morphological observations made from SEM. Due to the lack of high quality HRTEM, lattice fringes for silver and zinc oxide could not be measured to demonstrate diffusion of silver to the ZnO boundary.

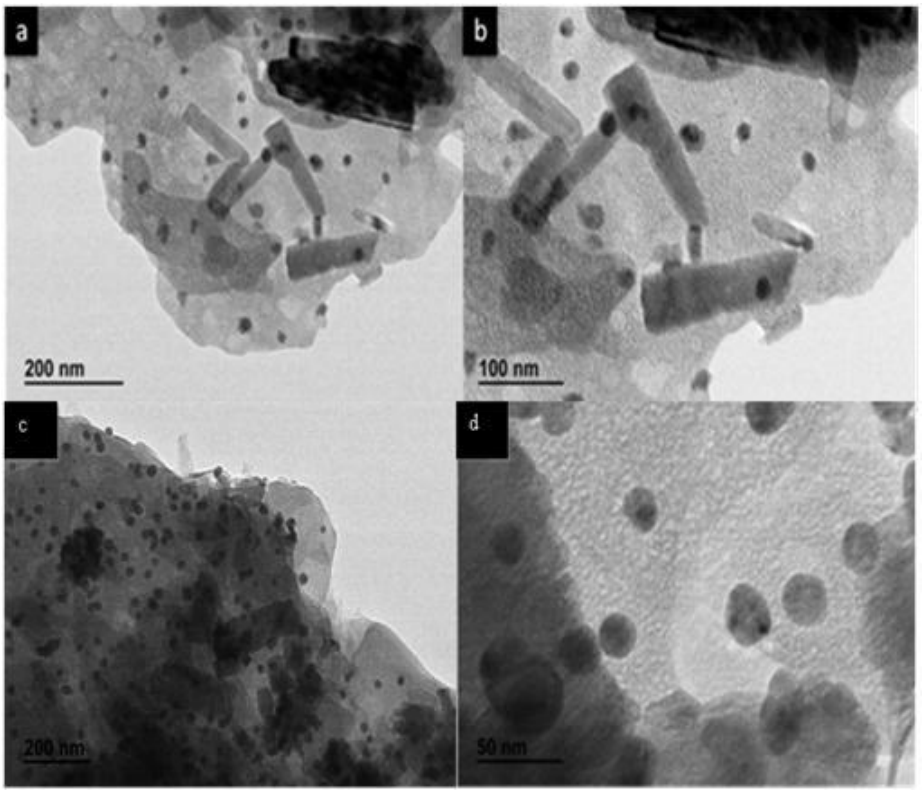

Figure 5: TEM images of as-prepared Ag/ZnO (a,b Ag/ZnO 1) (c, d Ag/ZnO 2)

XPS Analysis

We used XPS research to learn about the Ag/ZnO composite's surface components and chemical states. One possible conclusion is that, unlike undoped ZnO, which only contains Zn and O, Ag/ZnO only contains Ag, Zn, and O. The curves' calibration value is the carbon peak (C 1s) at 284.8. Zn 2p3/2 and Zn 2p1/2 are represented by the peaks at 1021.4eV and 1044.48eV, respectively, as seen in Figure 6. When Zn2+ ions are formed, it causes a splitting of the orbitals [21]. When silver is doped, the peak shows a little shift to a higher band energy. Two symmetrical signals, one representing lattice oxygen and the other surface hydroxyl oxygen, may accommodate the peak owing to oxygen O (1s) [16]. When oxygen is doped with Ag, it likewise exhibits a positive shift. There is a little departure from the bulk Ag value of 368.2 eV and 374.2 eV, respectively, and the distinctive peaks at 367.6 eV and 373.6 eV, which correspond to Ag 3d5/2 and 3d3/2, respectively, are given by silver. The reduction of Ag metal to form metallic silver is shown by the 6eV difference between two orbitals of Ag [18]. As the electron density of Ag decreases, the binding energy shifts to a lower value relative to pure silver. The reduction in the size of Ag's work function causes electron transport from the Ag layer to the ZnO surface's conduction band. This results in the formation of an energy level that signifies a strong contact between the Ag and ZnO particles. The interaction between zinc oxide and silver may explain why zinc and oxygen undergo positive shifts whereas silver undergoes negative shifts. The change to lower energy levels for silver must be due to the reduced binding energy of monovalent Ag compared to zerovalent Ag [39].

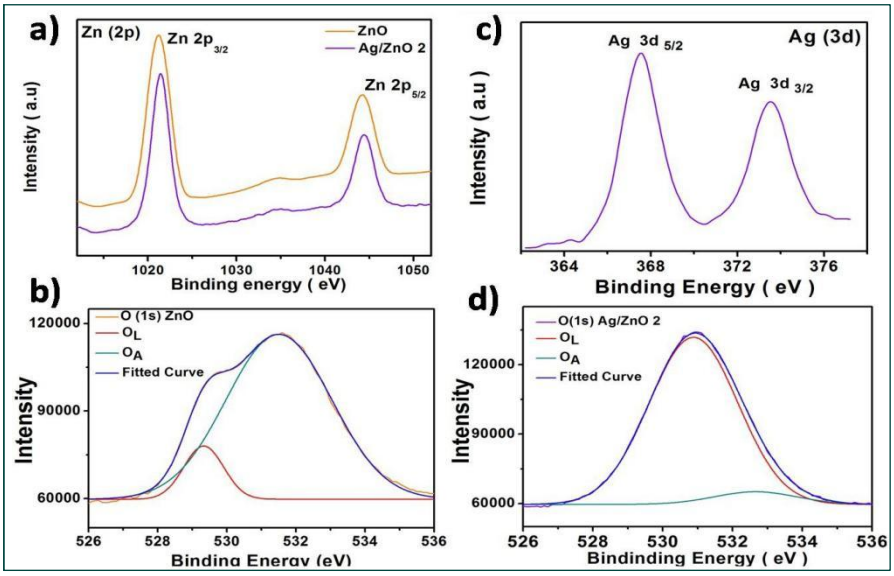

Figure 6: XPS patterns of ZnO and Ag/ZnO **2** a)Ag 3d spectrum b)Zn (2p) Oxygen spectrum of c) ZnO and d)Ag/ZnO **2**

UV/Vis Spectroscopy

The optical characteristics of Ag-doped ZnO nanoparticles were investigated using UV-Vis spectroscopy. A 373 nm peak, blue-shifted by about 10-15 nm relative to the bulk value, was produced by pure ZnO particles; this value is consistent with many others that have been reported. A little red shift in the ZnO peak is seen when the Ag nanoparticle is added to the ZnO. Figure 7a shows that the sample with the highest concentration of silver nanoparticles has an extra hump at 429 nm, which is caused by localized surface Plasmon resonance (LSPR). This hump may imply that the silver particles have a nearly spherical shape. When Ag is dissolved in ethanol, its LSPR peak is at 409 nm [40]. After being loaded into ZnO, the peak settles at 429 nm. This finding suggests a little amount of aggregation and an increase in particle size. There is a negative correlation between the metal's electron density and the Plasmon absorption peak [19]. Because of the redox reaction between zinc oxide and silver in the ZnO-O..Ag structural arrangement, the LSPR is likely to change. In order to reach Fermi level equilibrium, electrons will be transferred from the Ag band to the ZnO conducting band, due to the fact that silver has a lower work function than ZnO [37].

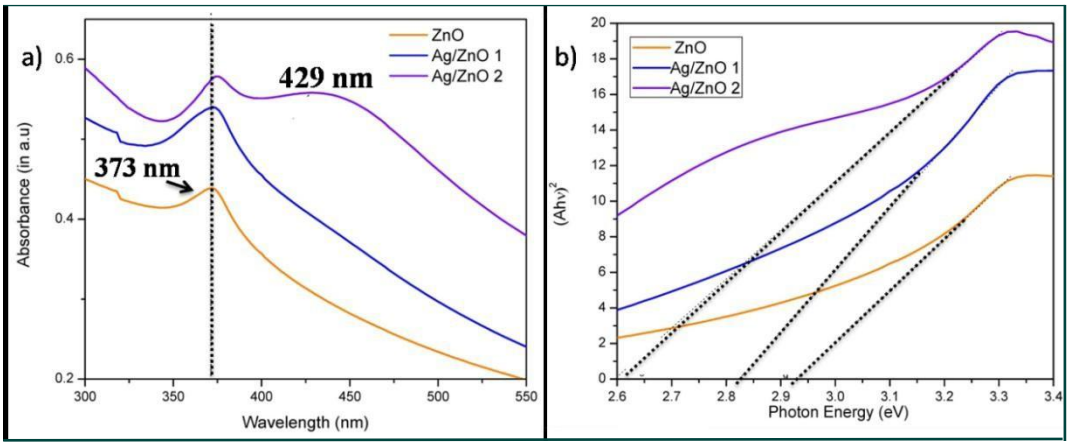

Figure 7: (a) UV/Vis Spectrum b) Tauc diagram of ZnO and Ag/ZnO samples

The hν values were plotted against $(\alpha h\nu)^2$ and extended to calculate the bandgap of the nanoparticles by Tauc method [36]. The band gap (Eg) of the ZnO was calculated to be 2.9 eV, however for the 1% and 4% Ag doped ZnO, a reduction was observed possibly due to oxygen richness on ZnO surfaces. Addition of Ag reduced the bandgap by about 0.1-0.3 eV to be observed at 2.8 eV and 2.6 eV. The reduced eV value enabled the possibility of high photoactivity of the nanoparticles in the visible region (Figure 7b).

Pholotolumiscence Spectra

To know more about the optical properties, Pholotolumiscence data of the samples is analyzed (Figure 8). PL spectrum can provide insights on quality of crystals, structural defects (surface oxygen vacancies, Zn interstitials) and particle surfaces [39]. The room temperature PL spectrum of the samples after exciting the absorption band at 325 nm is recorded. The strong emission peak at 389 nm is the main emission along with minor emissions at 493 and 530 nm which can be due to bound excitons and oxygen deficiency respectively [33]. PL intensity decreased as the concentration of Ag increased. Lower photoluminescence intensity is an indicator of higher life time of electron hole pair. It shows that the adding Ag into the ZnO matrix inhibits the recombination rate [41].

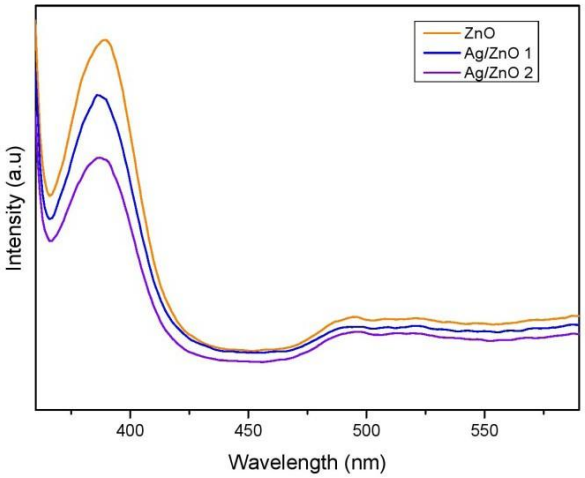

Figure 8: PL Spectra of ZnO and Ag/ZnO samples

Photocatalytic studies

The degradation of pollutants was done in direct sunlight at sunlight intensity of around 80000 lux (~590 W/m^2). Methylene Blue is a cationic Azo dye which has been widely studied as a model dye for monitoring photocatalytic reactions. Two major absorbance peaks of methylene blue in water were located at 292 nm and 664 nm, due to benzene ring and heteropolyaromatic linkage respectively. The peaks at 604 nm and 575nm are due to the formation of dimer and trimer particles of MB in aqueous condition [43]. Chemical structure of MB is given below (Figure 9a);

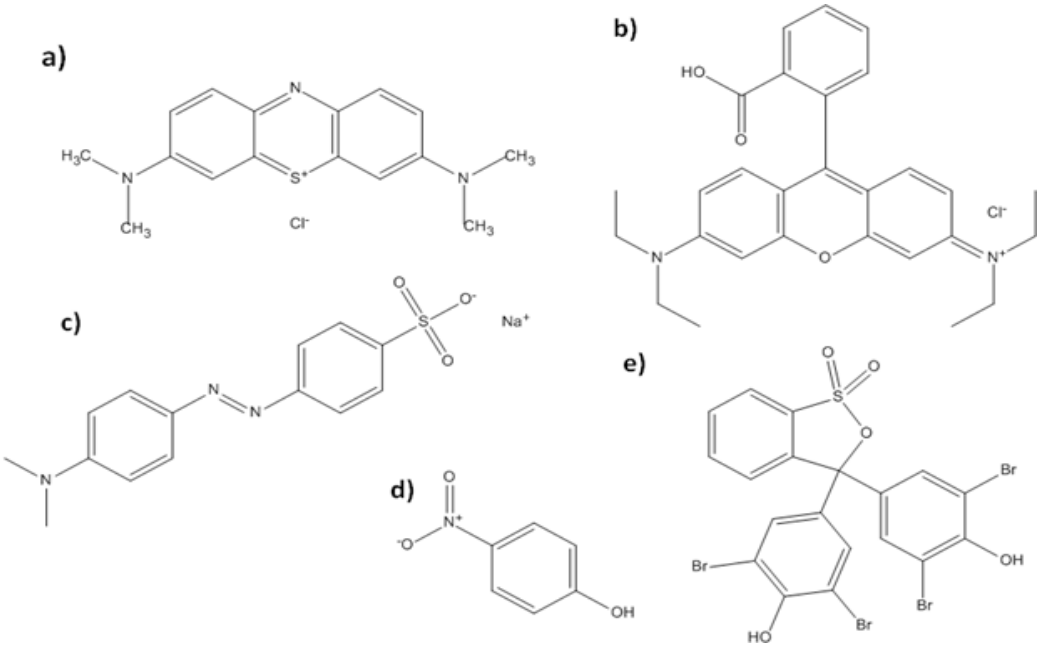

Figure 9: Chemical structure of dyes: a)Methylene Blue (MB) b)Rhodamine B (RhB), c)Methyl Orange (MO), d) p-nitrophenol (PNP) and e)Bromophenol Blue (BPB)

Under direct sunlight irradiation, the photocatalytic degradation of Methylene Blue was tested using produced ZnO NPs and Ag/ZnO NPs. As MB's absorption intensity (664 nm) changed, UV-vis spectroscopy tracked it in real time. The enzyme's photocatalytic capabilities are as follows: ZnO < Ag/ZnO 1 (1 wt %) < Ag/ZnO 2 (4 wt %). The rate was increased by 15% with 1% Ag/ZnO and by 40% with 4% Ag/ZnO. Figure 10 shows that MB decolorization in 120 minutes under direct sunshine irradiation with a catalyst concentration of 1.0 g L-1 and a concentration of 0.02 mM was accomplished in the presence of 4% Ag/ZnO. So, the development of a solar-light active ZnO and an exceptionally solar-light active Ag/ZnO photocatalyst have been validated. Every single sample has successfully degraded the Methylene Blue. In UV degradation curves, there are no obvious indications of intermediate generation. The increased degradation rate of the 664 nm peak in the reaction suggests that the monomers are degrading quicker. The following is a summary of the MB deterioration based on previously published literature:

$$C_{16}H_{18}N_3S + 24\,O_2 \rightarrow 16CO_2 + 3NO_3^- + SO_4^{2-} + 6H+ + 6H_2O \text{ [44]} \quad \text{.....(5)}$$

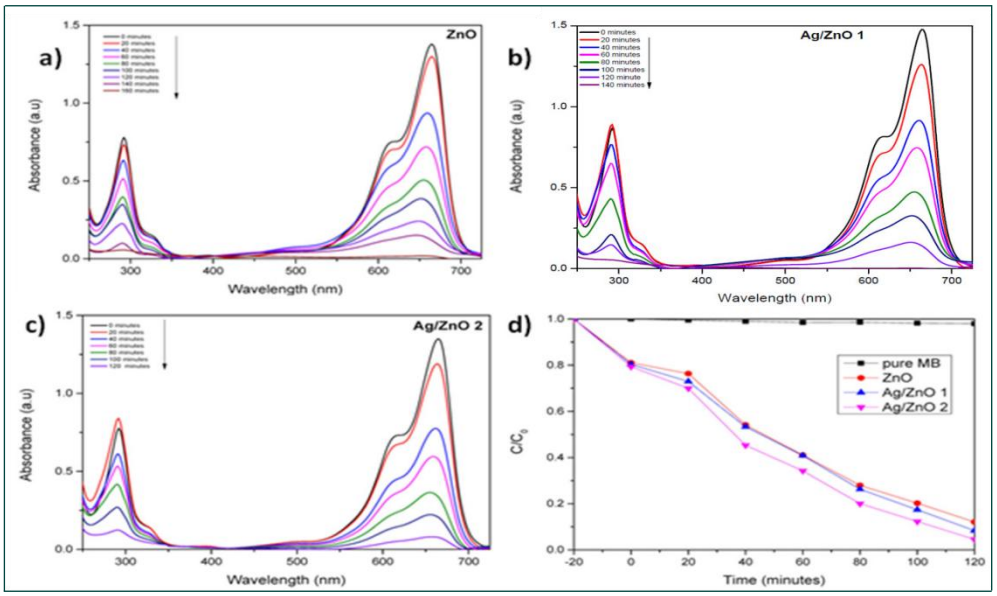

Figure 10: Degradation of MB with a) ZnO, b) 1% Ag/ZnO, c) 4% Ag/ZnO with 1.0g/Lcatalyst concentration d) C/C0 Vs time curves

The amount of catalyst required is another factor which influences the photocatalytic degradation of MB. The degradation rate was faster in reactions when the concentrations of catalyst (AgZnO) 0.5 g L^{-1} than 0.25 g L^{-1} (4%Ag). In fact the solution with the higher amount of the catalyst (1.0 g L^{-1}) should have offered more active surface area for the photocatalytic degradation of MB but surprisingly a decrease in the degradation rate was monitored which is presumably may be due to light scattering by excess amount of catalyst present [41] in the photocatalytic reaction system (Figure 11).

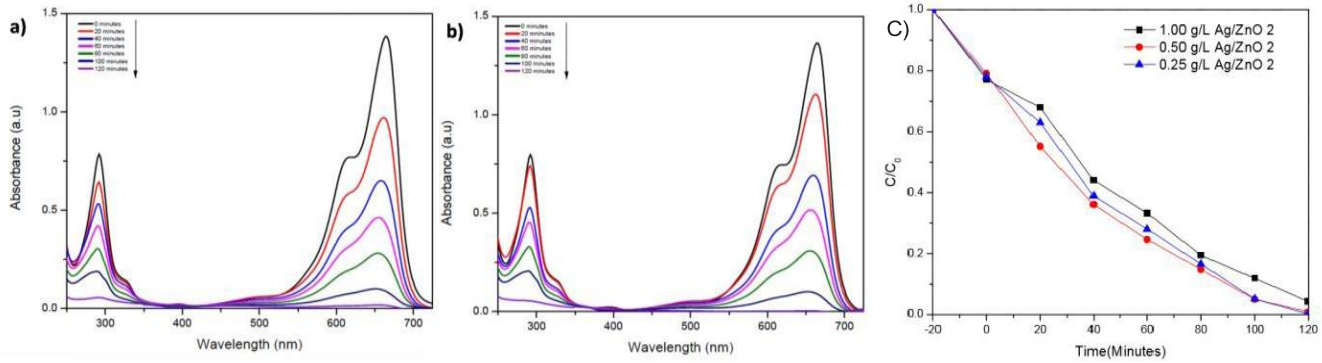

Figure 11: Degradation of MB with various concentrations of Ag/ZnO 2 a) 0.5g/l b)0.25g/l and c) C/C0 Vs time curves for degradation of MB with various concentration.

In order to study the reusability of the catalyst the reaction was repeated for four cycles. The catalyst remained highly solar active and retained around 95% of its activity. This confirms that the catalyst can be effectively used in photocatalytic reactors and can be used for commercial purposes, as the leaching of Ag in the surface is negligible (Figure 12).

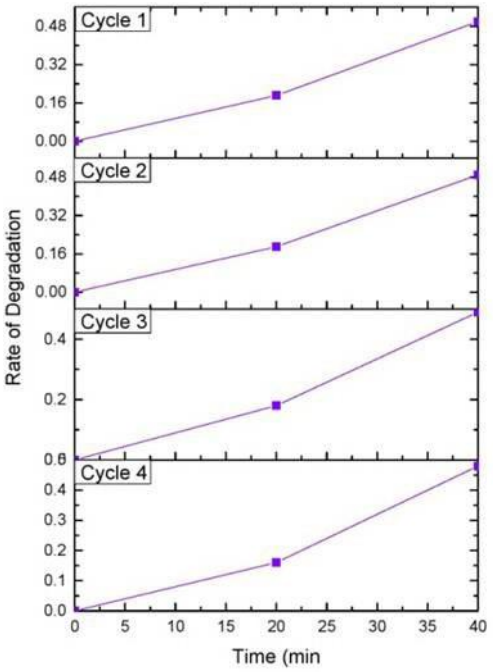

Figure 12: Recycle study of Ag/ZnO 2

In a similar vein, Figure 9b shows the results of testing Ag/ZnO's photcatalytic activities against Rhodamine B, another dye of significant commercial importance. In the case of Ag/ZnO, the Rhodamine B degradation reaction was quite rapid, taking just about 80 minutes to finish; in contrast, ZnO required twice that amount of time. Figure 13 I shows that the rate of degradation of cationic dyes may be further increased by adding silver to the ZnO matrix, even if the ZnO manufactured using the existing approach utilizing starch as a surface agent is already extremely efficient. In addition, the degradation of another industrially significant dye used in the textile sector was examined using the so-generated catalyst. Figure 9c shows that methyl orange, an anionic dye, may undergo catalytic reactions that separate it into organic compounds. With oxygen-rich surfaces and negative charges on the catalyst surface, the quantity of methyl orange absorbed by the catalyst is expected to be smaller [13]. Using ZnO as a catalyst alone resulted in inferior degradation (about 90% after 240 minutes). However, when silver was added to the ZnO, the degradation improved, demonstrating that the presence of silver allows anionic dye to be more effectively used.y are absorbed by the surface of the catalyst. Therefore, after 160 minutes, the whole reaction occurs (nearly 100%), in contrast to 240 minutes of radiation with ZnO

alone. Figure 13 II shows that planar ZnO outperformed several previously published research, providing further evidence that starch passivating ZnO surfaces may be successful on their own. The degradation of Bromophenol Blue, another anionic dye, was also examined with the two catalysts in this study. The reaction rate was faster for Ag/ZnO than for ZnO alone (Figure 14 I).

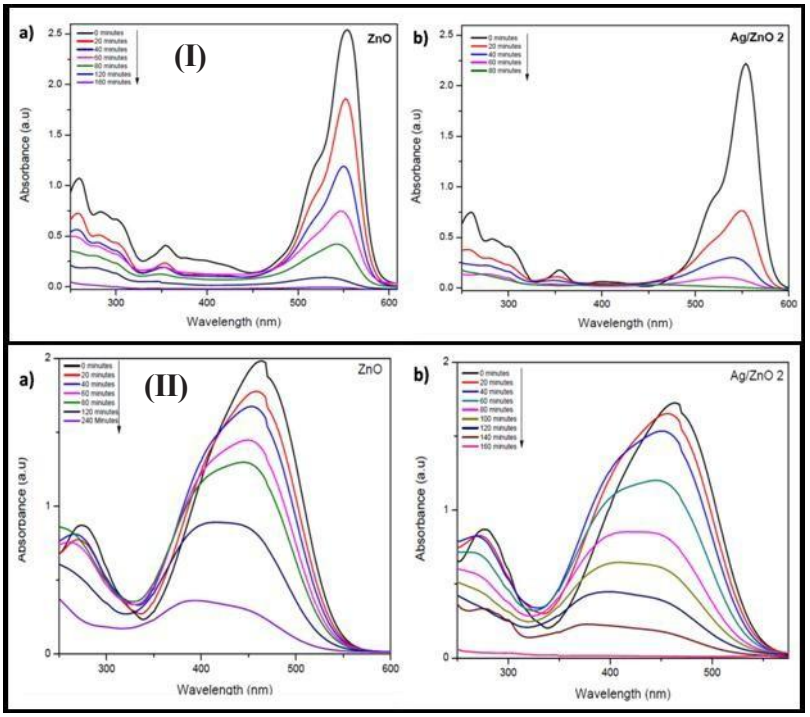

Figure 13: Photodegradation of (I) Rhodamine B, (II) MO using a) bare ZnO and b) Ag/ZnO 2

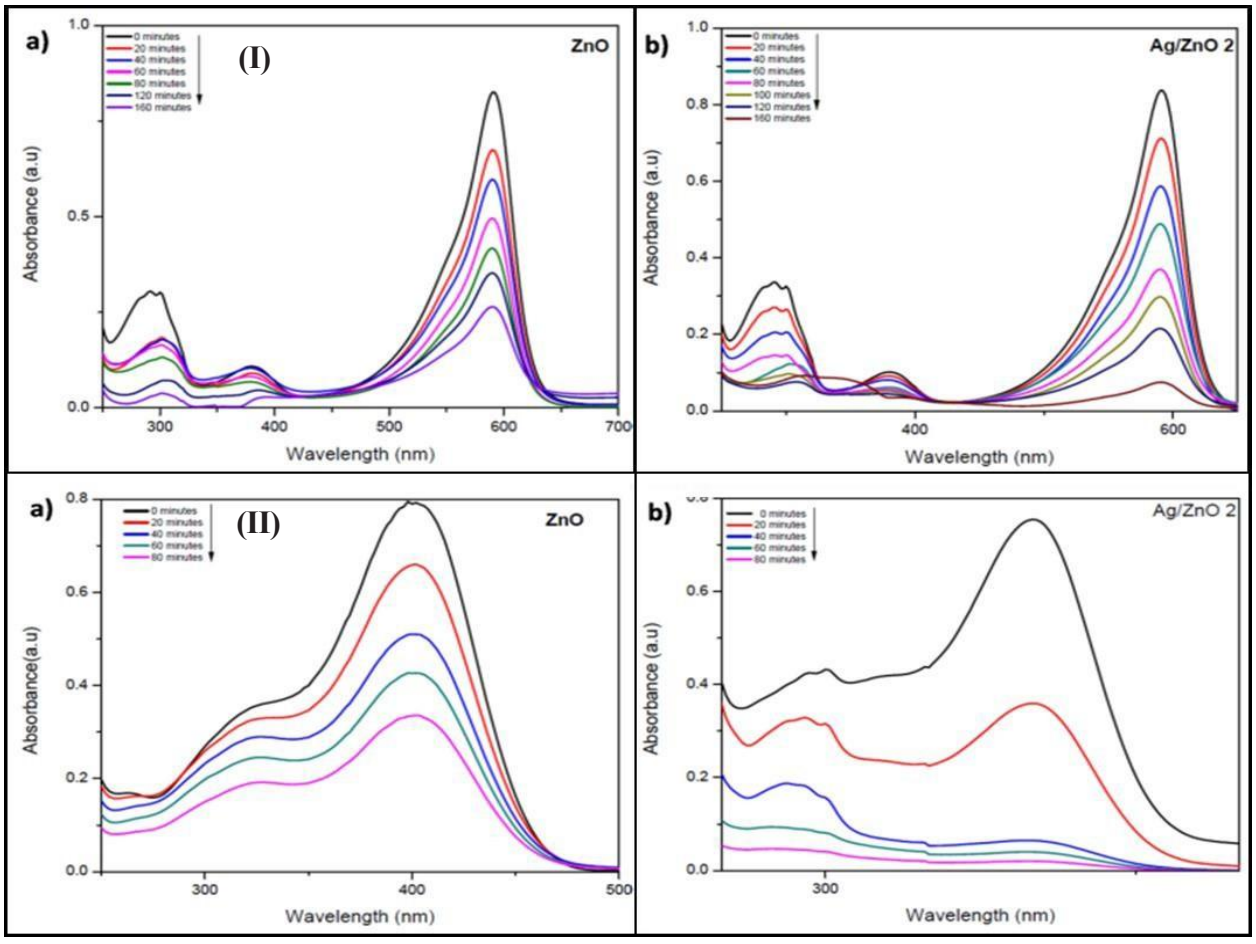

Figure 14: Degradation of (I) Bromophenol Blue, (II) p-nitrophenol using a) ZnO and b) Ag/ZnO **2**

Additionally, it is important in totality to understand need of effiuent treatment. There is large number of organic pollutants in industrial effiuent and providing a solution for total degradation of the contaminants, will obviously be a preferred technology. In order to establish the scope of current catalyst to have potential as a total solution, present article studies on phenol and phenolic compounds also which are common contaminants in industrial waste water. The degradation of phenols is challenging due to its stability and water solubility. For p-nitrophenol (Figure 9d) the reaction rates were very less for bare ZnO, the reaction was quite faster for Ag/ZnO. An intermediate peak, probably due to hydroquinone formation [45,46] is visible in the reaction for Ag/ZnO (Figure 14 II). By showing the efficiency of degradation for decomposition of five types of water pollutants, (Table 2) it is proposed that such type of catalyst can offer solution to water pollution problem that is a global concern.

Pollutants	Concentration of pollutants (mM)	Time for degradation (min)	Degradation (%) by	
			ZnO	Ag/ ZnO 2
Methylene Blue (MB)	0.02	120	90%	98%
Rhodamine B(RhB)	0.02	80	80%	99.9%
Methyl Orange(MO)	0.01	160	73%	98%
Bromophenol Blue (BPB)	0.005	160	64%	92%
p-nitrophenol (PNP)	0.01	80	70%	96%

Table 2: Efficiency of photocatalysts

Photocatalytic Mechanism

This research found that pure ZnO NPs exhibited strong photocatalytic activity. This is thought to be caused by two factors: first, the base material's high oxygen content narrowed the band gap, and second, dye sensitization excited the absorbed pollutant. Excess oxygen is evident in the catalyst sample, according to XPS and EDAX measurements. This is likely because starch has an oxidative function. A decrease in photocatalytic effectiveness may be seen when oxygen vacancies inside a ZnO crystal serve as recombination centers. Efficiency gains may be attributable to reduced recombination rates [2]. Possible low recombination rates and almost nonexistent impurity peaks are shown by the PL curve of ZnO. When exposed to visible light, chemisorbed dyes may be stimulated into single-and triple-states. To the conduction band of the semiconductor, electrons are transported from the excited dyes. Hydroxyl radicals are produced throughout the process and are responsible for advancing the degradation reaction [18]. Ag doping of ZnO results in the formation of nano hetero junctions. The superior photocatalytic activity of 4% Ag/ZnO (Ag/ZnO 2) compared to 1% Ag/ZnO (Ag/ZnO 1) seems to be due to the optimal loading of Ag, as shown by SEM and TEM measurements. Charge carrier recombination is prevented by the electrical interaction present in metal-semiconductor junctions. In a previous study, the authors found that Ag particles could absorb solar radiation by means of a localized surface plasmon resonance (LSPR) process, which in turn created an electric field that excited the electrons in the valence band of excited silver nanoparticles (Ag* in reaction 6) and transferred them to the conduction band of zinc oxide, resulting in the formation of zinc oxide (ZnO)(e) [5]. The present mechanism is comparable to this previous work. Afterwards, the charge will be transferred to Ag NPs by ZnO in Ag/ZnO, which speeds up the separation of photogenerated electron-hole pairs. Hydroxyl radicals are formed when holes in ZnO react with water, whereas superoxide (O.-) radicals are produced by electrons in the conduction band of Ag nanoparticles. The pollutant molecules are reduced to basic compounds by these radicals [42,47]. As shown in figure 15, the photocatalytic breakdown of MB in the presence of Ag/ZnO under sunlight is depicted schematically [41]. The typical procedure is as follows [19,48];

$Ag + h\upsilon \rightarrow Ag^{*}$ .....(6)

$Ag^{*} + ZnO \rightarrow Ag^{\bullet+} + ZnO(e)$ .....(7)

$ZnO(e) + O_2 \rightarrow ZnO + O_2^{\bullet-}$ .....(8)

$O_2^{\bullet-} + H+ \rightarrow \bullet OOH$ .....(9)

$\bullet OOH + ZnO(e) + H^{+} \rightarrow H_2O_2 + ZnO$ .....(10)

$H_2O_2 + ZnO(e) \rightarrow \bullet OH + OH^{-} + ZnO$ ..... (11)

Organic Pollutants + •OH (or •OOH) → Degraded Products .....(12)

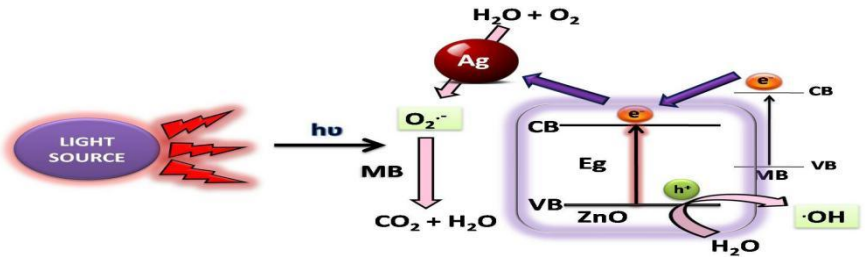

Figure 15: Proposed mechanism for degradation of MB *via* electronic events in presence of Ag/ZnO catalyst under sunlight

Additionally, in case of plasmonic photocatalyst (Ag/ZnO), intensive local electric field LSPR may create excitation of more electrons and holes and heat up the surrounding environment to increase the reaction rate and the mass transfer thereby polarizing the nonpolar molecules for better adsorption and absorption of pollutants with Ag/ZnO [30]. This local electric field may also have factored in better performance in the present study.

Conclusion

Starch was used to make an Ag/ZnO photocatalyst that is very efficient when exposed to sun light. During testing and assessment of its photocatalytic performance, the catalyst was characterized and found to have high crystalline characteristics as well as an excess of surface oxygen, both of which might be critical to the total catalytic activity. By increasing the band-gap towards the visible range, the presence of silver in the zinc oxide nanostructure transforms the UV-active zinc oxide into a visible light catalyst, allowing for its assessment under direct sunlight. There is evidence that silver improves photcatalysis and other surface qualities, such as dye absorption. In terms of catalyst ZnO, the photocatalytic activity was found to be best at 1 wt % Ag/ZnO 1 and 4 wt % Ag/ZnO 2, according to the comparative investigation. The rate was increased by 15% with 1% Ag/ZnO and by 40% with 4% Ag/ZnO. The Ag/ZnO 2 photocatalyst had the best performance (99.9% efficiency) when tested against rhodamine B. Methylene blue and rhodamine B were cationic dyes, whereas methyl orange, bromophenol blue, and p-nitrophenol were anionic dyes, all of which may be degraded by the catalysts that were thus produced. Even after the third cycle, it continued to exert its effects. An increase in the catalyst's potential industrial uses is the fact that it may be employed directly in sunlight.

References

1. The Electrochemical Photolysis of Water at a Semiconductor Electrode by Fujishima and Honda (1972). Page 37–38 of Nature 238. The authors of the 2011 paper "Oxygen Rich Titania: A Dopant Free, High Temperature Stable, and Visible Light Active Anatase Photocatalyst" are Etacheri, Seery, Hinder, and Pillai. Academic Journal of Functional Materials, 21(21), 3744–3752, 2017.b) "One-dimensional-based spatially ordered architectures for solar energy conversion" developed by Liu S, Tang ZR, Sun Y, Colmenares JC, and Xu YJ in 2015. The chemical society review, volume 44, pages 5053–5075. 3. A study conducted by Jag YJ, Simer C, and Ohm T (2006) compared the photocatalytic degradation of methylene blue using zinc oxide nanoparticles and its nano-crystalline particles. Mater Physical Review B, 41, 67–77. 4. a) Li et al. (2008) tested the photocatalytic degradation of phenol on TiO2 and ZnO in the presence of manganese dioxides; the results were compared. (Catal Today 139: 109–112). b) In 2015, Zhang et al. took a waltz using graphene as a platform to create composite photocatalysts. Yang, Liu, Sun, and Xu were the authors. Research in Chemistry 115: 10307–77. X. Zhou, G. Liu, J. Yu, and W. Fan (2012) Luminescent surface plasmon resonance photocatalysis using composites based on noble metals. Applied Mater. Sci. 22: 21337-84. The authors Primo, Corma, and García (2011) used titanium as a photocatalyst with gold nanoparticles. Phys Chem "Chemistry and Physics" 13: 886–9010. 7. Collado L., Jana P., Sierra B., Coronado J., Pizarro P., et al. (2013). Synergistic impact of Ag supported on TiO2 and ZnO semiconductors enhances hydrocarbon production by artificial photosynthesis. Citation: Chem Eng J 224: 128-35. Branched TiO2 nanorods for photoelectrochemical hydrogen generation. Nano lett 11: 4978-84. 8. Cho IS, Chen Z, Forman AJ, Kim DR, Rao PM, et al. (2011). 9. Ravishankar T, Manjunatha K, Ramakrishnappa T, Nagaraju G, Kumar D, et al. (2014). Zinc oxide nanoparticles doped with silver and those without were compared for their photocatalytic degradation of trypan blue. The article is published in Mater Sci Semicon Proc 36: 7-17. 9. In a 2014 study, Jasso-Salcedo, Palestino, and Escobar-Barrios developed Time, pH, and Ag on the formation of zinc oxide nanoagglomerates functionalized with Ag as photocatalysts. Published in the Journal of Catal Science 318: 170-8. 11. Wang Y, Wang Q, Zhan X, Wang, Safdar M, et al. (2013) Type II heterostructures powered by visible light and their improved photocatalytic capabilities: a comprehensive look. Nanoscale5, 8326–8339. 12. Mekasuwandumrong O, Praserthdam P, Pratsinis SE, and Height MJ (2006) Developed Ag-ZnO catalysts for UV-photodegradation of methylene blue. Thirteen. Rauf M, Ashraf SS (2009) Basic concepts and practical uses of heterogeneous photocatalytic dye degradation in solution. Appl Catal B-Environ 63: 305-12. The photocatalytic breakdown process of methylene blue in water was described by Houas et al. (2001) in Chem Eng J 151: 10-8. Environmental

and Applied Catalysis 31: 145–57. 15. Methods for activating TiO2 and ZnO with visible light, by Rehman, Ullah, Butt, and Gohar (2009). Scientific Reports, Part 170: 560–569. 16. The band-gap narrowing and improved visible light photocatalytic activity of ZnO produced by oxygen vacancies was reported by Wang J, Wang Z, Huang B, Ma Y, Liu Y, and colleagues in 2012. 17, ACS Applied Materials Interfaces 4: 4024-30. The authors of the 2007 article "Ag/ZnO heterostructure nanocrystals: synthesis, characterization, and photocatalysis" are Zheng Y, Zheng L, Zhan Y, Lin X, and Zheng Q. Organic Chemistry, 46, 6980–6906. 18. The improved photocatalytic activities of Ag nanoparticle decorated nanoporous ZnO microrods were reported by Deng Q, Duan X, Ng DH, Tang H, Yang Y, and colleagues in 2012. Journal of Advanced Chemical Materials, Volume 4, Issues 6030–6037, 2019. Researchers Han, Ren, Cui, Chen, Pan, and others (2012) used Ag/ZnO floral heterostructures powered by visible light by surface plasmon resonance as a photocatalyst. Methods in Catalysis Part B—Environment 126: 298-305. 20. Authors Li Y, Zhao X, and Fan W. (2011) conducted a first principles investigation on the optical, electrical, and structural characteristics of Ag-doped ZnO nanowires. The reference for this article is J. Phys. Chem. C 115: 3552–7527. 21. A paper titled "Facile synthesis of sheet-like ZnO assembly composed of small ZnO particles for highly efficient photocatalysis" was published in 2013 by Hong Y, Tian C, Jiang B, Wu A, Zhang Q, and others. The citation is from the Journal of Materials Chemistry, volume 1, pages 5700–5708. 22.a.) A soluble starch-assisted approach for the facile production of monodisperse porous ZnO spheres and their photocatalytic activity was described by Zhang G, Shen X, and Yang Y in 2011. Journal of Physical Chemistry C, Volume 115, Pages 7145–752, 2007. b) Khanna PK, Singh N, Kulkarni D, Deshmukh S, Charan S, et al. (2007) Simple production of re-dispersible silver nanoparticles using water. Journal of Materials Research 61: 3366–3370 (c) Khanna PK, Bhagat UK, More PV Research on Nanofluids of Zinc Oxide for Use in Heat Transfer (2015). SAJ "Synthesis of nano-particles of anatase TiO2 and preparation of its optically transparent film in PVA" (Nanoscience and Nanotechnology, 2007, 101). Publication: Materials Letters 61: 4725-30. Producing and maintaining metal nanoparticles in an entirely "green" manner was the subject of Raveendran et al. (2003). In the Journal of the American Chemical Society, volume 125, pages 13940-1. Section 24: Lin, Thirumavalavan, Jiang, and Lee (JF) In 2014, researchers synthesized a ZnO/Zn nano photocatalyst for dye photodegradation utilizing modified polysaccharides. The authors of the 2013 article "Starch-stabilized synthesis of ZnO nanopowders at low temperature and optical properties study" published in Carbohyd Polym (105: 1-9), Majid WA, Mahmoudian M, Darroudi M, and Yousefi R. Adv Power Tech 24: 618-24.
b) In 2006, Ye et al. reported that the photocatalytic efficacy of ZnO nanoplatelets depends on their thickness. J Scientific American, 110, 15146–151. c) Makarova OV, Rajh T, Thurnauer MC, Martin A, Kemme PA, et al. (2000) Surface modification of TiO2 nanoparticles for photochemical reduction of nitrobenzene. Nature Science & Technology 34: 4797-803. 26. a) Xie S, Lu X, Zhai T, Li W, Yu M, et al. (2012) Enhanced photoactivity and stability of carbon and nitrogen co-treated ZnO nanorod arrays for photoelectrochemical water splitting. Published in the Journal of Materials Chemistry, volume 22, pages 14272-52.
b) Han C, Yang MQ, Weng B, Xu YJ (2014) Improving the photocatalytic activity and anti-photocorrosion of semiconductor ZnO by coupling with versatile carbon. Phys Chem Chem Phys 16: 16891-903.
c) Weng B, Yang MQ, Zhang N, Xu YJ (2014) Toward the enhanced photoactivity and photostability of ZnO nanospheres via intimate surface coating with reduced graphene oxide. J Mater Chem A 2: 9380-9.
27. Ahmad M, Ahmed E, Zhang Y, Khalid N, Xu J, et al. (2013) Preparation of highly efficient Al-doped ZnO photocatalyst by combustion synthesis. Curr Appl Phys 13: 697-704. 28. Liu S, Li C, Yu J, Xiang Q (2011) Improved visible-light photocatalytic activity of porous carbon self-doped ZnO nanosheet-assembled flowers. Cryst Eng Comm 13: 2533-41. 29. Vignesh K, Suganthi A, Rajarajan M, Sara S (2012) Photocatalytic activity of AgI sensitized ZnO nanoparticles under visible light irradiation. Powd Technol 224: 331-7. 30. Zhang X, Chen YL, Liu R-S, Tsai DP (2013) Plasmonic photocatalysis. Rep Prog Phys 76: 046401.
31. Awazu K, Fujimaki M, Rockstuhl C, Tominaga J, Murakami H, et al. (2008) A plasmonic photocatalyst

consisting of silver nanoparticles embedded in titanium dioxide. J Am Chem Soc 130: 1676-80. 32. Dao TD, Han G, Arai N, Nabatame T, Wada Y, et al. (2015) Plasmon-mediated photocatalytic activity of wet-chemically prepared ZnO nanowire arrays. Phys Chemi Chem Phys 17: 7395-403. 33. Georgekutty R, Seery MK, Pillai SC (2008) A highly efficient Ag-ZnO photocatalyst: synthesis, properties, and mechanism. J Phys Chem C 112: 13563-70. 34. Mondal C, Pal J, Ganguly M, Sinha AK, Jana J, et al. (2014) A one pot synthesis of Au–ZnO nanocomposites for plasmon-enhanced sunlight driven photocatalytic activity. New J Chem 38: 2999-3005. 35. Liu Y, Wei S, Gao W (2015) Ag/ZnO heterostructures and their photocatalytic activity under visible light: Effect of reducing medium. J Hazard Mater 287: 59-68. 36. Yıldırım OA, Unalan HE, Durucan C (2013) Highly Efficient Room Temperature Synthesis of Silver-Doped Zinc Oxide (ZnO:Ag) Nanoparticles: Structural, Optical, and Photocatalytic Properties. J Am Ceram Soc 96: 766-73. 37. a) Ansari SA, Khan MM, Ansari MO, Lee J, Cho MH (2013) Biogenic synthesis, photocatalytic, and photoelectrochemical performance of Ag–ZnO nanocomposite. J Phys Chem C 117: 27023-30, b) Pan X, Yang MQ, Fu X, Zhang N, Xu Y-J (2013) Defective TiO2 with oxygen vacancies: synthesis, properties and photocatalytic applications. Nanoscale 5: 3601-14. c) X Pan, Yang MQ, Xu YJ (2014) Morphology control, defect engineering and photoactivity tuning of ZnO crystals by graphene oxide – a unique 2D macromolecular surfactant. Phys Chem Chem Phys 16: 5589-99. 38. Vayssieres L (2003) Growth of arrayed nanorods and nanowires of ZnO from aqueous solutions. Adv Mater 15: 464-6. 39. Sun F, Qiao X, Tan F, Wang W, Qiu X (2012) One-step microwave synthesis of Ag/ZnO nanocomposites with enhanced photocatalytic performance. J Mater Sci 47: 7262-8. 40. Pal A, Shah S, Devi S (2009) Microwave-assisted synthesis of silver nanoparticles using ethanol as a reducing agent. Mater Chem Phys 114: 530-2. 41. Kaviya S, Prasad E (2015) Biogenic synthesis of ZnO–Ag nano custard apples for efficient photocatalytic degradation of methylene blue by sunlight irradiation. RSC Adv 5: 17179-185. 42. Liu X, Li W, Chen N, Xing X, Dong C, et al. (2015) Ag-ZnO heterostructure nanoparticles with plasmon-enhanced catalytic degradation for Congo red under visible light. RSC Adv 5: 34456-65. 43. Heger D, Jirkovsky J, Klan P (2005) Aggregation of methylene blue in frozen aqueous solutions studied by absorption spectroscopy. J Phys Chem A 109: 6702-9. 44. Lachheb H, Puzenat E, Houas A, Ksibi M, Elaloui E, et al. (2002) Photocatalytic degradation of various types of dyes (Alizarin S, Crocein Orange G, Methyl Red, Congo Red, Methylene Blue) in water by UV-irradiated titania. Appl Catal B-Environ 39: 75-90. 45. Maurino V, Minero C, Pelizzetti E, Piccinini P, Serpone N, et al. (1997) The fate of organic nitrogen under photocatalytic conditions: degradation of nitrophenols and aminophenols on irradiated TiO2. J Photochem Photobiol A 109: 171-6. 46. Nagaveni K, Sivalingam G, Hegde M, Madras G (2004) Photocatalytic degradation of organic compounds over combustion-synthesized nano- TiO2. Environ Sci Technol 38: 1600-4.47. Xiao M, Jiang R, Wang F, Fang C, Wang J, et al. (2013) Plasmon-enhanced chemical reactions. J Mater Chem A 1: 5790-805. 48. Kochuveedu ST, Jang YH, Kim DH (2013) A study on the mechanism for the interaction of light with noble metal-metal oxide semiconductor nanostructures for various photophysical applications. Chem Soc Rev 42: 8467-93.

1.